49th IEEE Conference on Decision and Control
December 15-17, 2010
Hilton Atlanta Hotel, Atlanta, GA, USA

Nonlinear Model Predictive Control for Power-split Hybrid Electric Vehicles

H. Ali Borhan, Chen Zhang, Ardalan Vahidi, Anthony M. Phillips, Ming L. Kuang, and S. Di Cairano

Abstract*— In this paper, a causal optimal controller based on Nonlinear Model Predictive Control (NMPC) is developed for a power-split Hybrid Electric Vehicle (HEV). The global fuel minimization problem is converted to a finite horizon optimal control problem with an approximated cost-to-go, using the relationship between the Hamilton-Jacobi-Bellman (HJB) equation and the Pontryagin's minimum principle. A nonlinear MPC framework is employed to solve the problem online. Different methods for tuning the approximated minimum cost-to-go as a design parameter of the MPC are discussed. Simulation results on a validated high-fidelity closed-loop model of a power-split HEV over multiple driving cycles show that with the proposed strategy, the fuel economies are improved noticeably with respect to those of an available controller in the commercial Powertrain System Analysis Toolkit (PSAT) software and a linear time-varying MPC controller previously developed by the authors.

I. Introduction

A Hybrid Electric Vehicle (HEV) combines the mechanical energy produced by a combustion engine with the electrical energy of an energy storage system (usually a battery), hence providing extra degrees of freedom for operating the engine more efficiently. Another benefit of an HEV comes from its ability to capture the kinematic energy of the vehicle which is normally wasted during braking. Among different HEV configurations, the power-split type is the most versatile one having been used by several auto-makers. The Toyota Prius, Ford Escape, and Ford Fusion hybrids are all power-split HEVs currently in production. The versatility provided by a planetary gear set (a speed coupler) in a powerplit hybrid allows the engine operation to be completely decoupled from the vehicle motion. Also, the battery can assist the engine or it can store part of the mechanical energy from the engine or from braking. The challenge is to decide how to split the driver's demanded power between the engine and the battery and to select the system operation point such that the fuel consumption is minimized without sacrificing drivability.

The fuel minimization problem of an HEV is a nonlinear and constrained optimal control problem. Assuming full knowledge of the future driving conditions, the globally optimal solution for a model of the HEV can be derived using dynamic programming (DP). However the DP solution is noncausal due to its dependence on (generally unknown) future power demands and it is computationally demanding when a long horizon is considered. The DP solutions over the known driving conditions have been used mainly as benchmarks for the best achievable fuel economies [1]. By defining an equivalent fuel cost for the battery energy, Equivalent Fuel Consumption Minimization (ECMS) methods have been developed and solved at each instant rather than over driving interval [2], [3], [4]. Although ECMS can be applied online as a closed-loop controller, the decisions may be very short-sighted because the dynamics of the system (battery in general) are considered instantaneous.

A compromise between the computational cost and the non-causality of a globally optimal DP solution and the faster, causal, but instantaneous ECMS solution can be formed in an energy management strategy based on the Model Predictive Control (MPC) where a finite horizon is taken into account. In [5], a linear-time varying MPC (LTV MPC) framework [6] with a quadratic cost functional for the energy management was developed and it was applied to a closed-loop model of a power-split HEV. Although the LTV MPC results were comparable with a well-tuned controller of PSAT software [7], there seemed to be room for further improvement in the fuel economy. In this paper, we reformulate the MPC fuel minimization problem to include not only the finite horizon cost of fuel but an approximate cost-to-go beyond the planning horizon represented as a terminal cost in the MPC finite horizon optimization problem . We use the relationship between the Hamilton-Jacobi-Bellman (HJB) equation and the Pontryagin's minimum principle ([8]), to show that the fuel cost-to-go can be approximated as a linear function of deviations in the battery's state of charge. Our derivations support the results published in [9] parallel to our research. A nonlinear MPC framework is employed to solve the optimal control problem online. Simulation results on a closed-loop model of a power-split HEV with respect to both the previous LTV MPC and the PSAT software show noticeable improvements.

II. The Plant Model

In the closed-loop simulations in this paper, we use a detailed model for a powersplit HEV from the database of Powertrain Simulation Analysis Toolkit (PSAT) commercial software [7]. PSAT is a state-of-the-art flexible powertrain simulation software developed by Argonne National Laboratory with the support of automotive manufacturers and sponsored by the U.S. Department of Energy (DOE). It runs in a MATLAB/Simulink environment and provides access to dynamic models of different mechanical and electrical components of several hybrid vehicle configurations. The level of details in PSAT component models and its forward simulation approach ensures reliable estimation of fuel economy. The modeling accuracy of PSAT has been validated against production HEVs such as Honda Insight [10] and

Ali Borhan, Chen Zhang, and Ardalan Vahidi are with the Dept. of Mechanical Engineering, University of Clemson. {hborhan, chenz, and avahidi}@clemson.edu Anthony M. Phillips, Ming L. Kuang, and Stefano Di Cairanois are with Ford Motor Company, Dearborn, MI. {aphilli8, mkuang, and sdicaira}@ford.edu

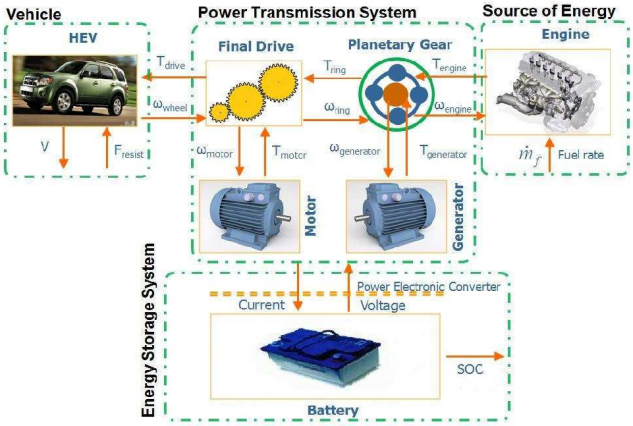

Fig. 1. A Power-Split HEV Configuration

Toyota Prius [11]. In order to analyze the performance of our MPC power management scheme on a high-fidelity dynamic model of a power-split HEV, the PSAT Simulink model of the Toyota Prius was chosen as the plant model for the closed-loop simulations. The MPC module receives all the feedback signals from this model and issues its engine torque and speed commands to the PSAT model. Because the PSAT model is too complex for control design, a simplified control-oriented model that captures the details that are of importance for the supervisory energy management scheme is derived and presented in this section. Figure 1 shows various subsystems of a powersplit hybrid and their interactions. More details are available in [12], [13], and [5].

The battery's state of charge SOC is the main dynamic state in optimal control of HEV's [1] and its dynamics can be described by [14],

$$\frac{dSOC}{dt} = -\frac{V_{oc} - \sqrt{V_{oc}^2 - 4P_{batt}R_{batt}}}{2C_{batt}R_{batt}}, \tag{1}$$

where

$$P_{batt} = P_{mot} + P_{gen} + P_{motor}^{loss} + P_{gen}^{loss}. \tag{2}$$

In these equations, V_{oc}, R_{batt}, and C_{batt} are the battery's open-circuit voltage, internal resistance, and capacity, respectively; P_{batt} is the battery power; P_{mot} and P_{gen} are the motor and generator powers; and P_{motor}^{loss} and P_{gen}^{loss} are the motor and generator power losses, respectively. In this model, positive power indicates battery discharging and negative power indicates battery charging. Empirical maps, extracted from PSAT, are used to calculate the power losses of motor and generator as functions of their torque and speed.

The power transmission system which is also called electric-continuously variable transmission, includes a planetary gear set (speed coupler) which combines the powers of the engine, motor, and generator. The energy coupling is accomplished in a way that the engine operation is decoupled from the vehicle. Neglecting the inertia of pinion gears in the planetary gear set and assuming all connecting shafts in the power transmission are rigid, the dynamics of the transmission can be obtained using Newton's laws [5],

$$\begin{aligned} J_{gen}\frac{d\omega_{gen}}{dt} &= T_{gen} + F \times N_S \\ J_{eng}\frac{d\omega_{eng}}{dt} &= T_{eng} - F \times (N_S + N_R) \\ J_{mot}\frac{d\omega_{mot}}{dt} &= T_{mot} - \frac{T_{out}}{g_f} + F \times N_R, \end{aligned} \tag{3}$$

where J_{eng} is the lumped inertia of the engine and the carrier gear; J_{gen} is the lumped inertia of the generator and the sun gear; and J_{mot} is the inertia of the motor lumped with the inertias of the ring, final transmission, and wheels. In (3), N_S and N_R are the radii of the sun and ring gears; T_{eng}, T_{gen}, and T_{mot} are the engine, generator, and motor torques, respectively; ω_{eng}, ω_{gen}, and ω_{mot} are the engine, generator, and motor speeds, respectively; and T_{out} is the output torque of the power transmission system. Finally in (3), F is the interaction force between the different parts of the gear set. To reduce the number of dynamic states, the inertial losses of the engine, motor, and generator, i.e. $J_{eng}\frac{d\omega_{eng}}{dt}$, $J_{mot}\frac{d\omega_{mot}}{dt}$, and $J_{gen}\frac{d\omega_{gen}}{dt}$, are ignored in the control-oriented model. This reduces the relationships in equation (3) to three static equality constraints. Furthermore, an empirical map of the engine, extracted from PSAT software, is used to relate the fuel flow rate, $\dot{m}_f$, to the engine speed and torque. There are also two kinematic equality constraints between velocities,

$$N_s\omega_{gen} + N_R\omega_{mot} = (N_s + N_R)\,\omega_{eng} \tag{4}$$

$$\omega_{mot} = \frac{g_f}{r_w}V, \tag{5}$$

where V is the vehicle velocity. The vehicle velocity is another state of the HEV model and its dynamics can be modeled by,

$$m\frac{dV}{dt} = \frac{T_{out} + T_b}{r_w} - \frac{1}{2}\rho A_f C_d V^2 - C_R mg\cos(\theta) + mg\sin(\theta). \tag{6}$$

In (6), m and A_f are the mass and frontal area of the vehicle, respectively; r_w is the wheel radius; C_R is the rolling resistance coefficient; C_D and ρ are the drag coefficient and air density, respectively; g_f is the final derive ratio; θ is the road grade which is assumed to be positive when vehicle goes down; and g is the gravity acceleration. The drivability constraint requires that the total torque at the wheels, which is the sum of the powertrain torque T_{out} and the friction brake torque T_b, is equal to the driver demanded torque T_{driver},

$$T_{out} + T_b = T_{driver}. \tag{7}$$

Considering the drivability constraint (7), the vehicle speed dynamics (6) does not add a control state for the energy management problem. But this dynamics will be used later for the estimation of the vehicle velocity over the MPC prediction horizon.

There are also several physical constraints, generally time-varying, that should be enforced. For the HEV power management, the constraints are,

$$\begin{aligned} SOC^{\min} \le SOC \le SOC^{\max};\ P_{batt}^{\min} \le P_{batt} \le P_{batt}^{\max} \\ \omega_{eng}^{\min} \le \omega_{eng} \le \omega_{eng}^{\max};\ T_{eng}^{\min} \le T_{eng} \le T_{eng}^{\max} \\ T_{mot}^{\min} \le T_{mot} \le T_{mot}^{\max};\ \omega_{mot}^{\min} \le \omega_{mot} \le \omega_{mot}^{\max} \\ T_{gen}^{\min} \le T_{gen} \le T_{gen}^{\max};\ \omega_{gen}^{\min} \le \omega_{gen} \le \omega_{gen}^{\max} \end{aligned} \tag{8}$$

where $\cdot^{\min}$ and $\cdot^{\max}$ denote the minimum and maximum bounds which are generally variable.
The outputs of the model are divided into tracking outputs (y_r) and constraint outputs (y_c),

$$y_r = \begin{bmatrix} SOC \\ \dot{m}_f \end{bmatrix}, \quad y_c = \begin{bmatrix} P_{batt} \\ \omega_{gen} \\ T_{mot} \\ T_{gen} \end{bmatrix}$$

Based on the above assumptions, the control oriented model can be represented by,

$$\begin{aligned} \dot{x} &= f(x,u,v) \\ y_r &= g_r(x,u,v) \\ y_c &= g_c(x,u,v) \end{aligned} \tag{9}$$

where

$$x = SOC, \quad u = \begin{bmatrix} T_{eng} \\ \omega_{eng} \end{bmatrix}, \quad v = \begin{bmatrix} T_{driver} \\ V \end{bmatrix},$$

x is the dynamic state, u is the control input, and v is defined as the measured disturbances to the model which are known at each time but not known for the future.

III. The Fuel Minimization Problem

The total fuel cost over an entire cycle which starts at time t_0 and ends at time t_f can be written as,

$$J = \int_{t_0}^{t_f} \dot{m}_f(u(t))dt + h(SOC(t_f)) \tag{10}$$

where $h(SOC(t_f))$ penalizes the deviation of SOC at the end of the cycle from a reference value, SOC_r. The objective of the power management strategy is to minimize the cost function (10) while satisfying the dynamical equations (9) and the constraints (8). However in the real applications, the driving conditions over long time horizons are not generally known in advance and furthermore, the parameters of the model and of the constraints may vary. Moreover, the solution of the optimal control problem over a long horizon is computationally demanding. To remedy these issues, we propose to use Bellman's Principle of Optimality to break the above optimal control problem in a (integrated) stage cost and an approximated minimum fuel cost from the end of the horizon to the end of the drive cycle and to solve the obtained problem in a receding horizon framework.
At time $t \le t_f$ during the travel, the cost function is,

$$J(u,SOC(t),t) = \int_{t}^{t_f} \dot{m}_f(u(\sigma))d\sigma + h(SOC(t_f)) \tag{11}$$

where $SOC(t)$ is any admissible state value at t. Notice that the performance measure depends on the values of $SOC(t)$, t, and the control history over the interval $\left[\ t \quad t_f\ \right]$. The minimum cost or cost-to-go is obtained by,

$$J^*(SOC(t),t) = \min_{\substack{u(\sigma) \\ t\le\sigma\le t_f}} \{ \int_{t}^{t_f} \dot{m}_f(u(\sigma))d\sigma + h(SOC(t_f)) \} \tag{12}$$

subject to the physical constraints (8) and dynamics (9). By subdividing the time interval one can write,

$$\begin{aligned} J^*(SOC(t),t) = \min_{\substack{u(\sigma) \\ t\le\sigma\le t_f}} \{ \int_{t}^{t+\Delta t} \dot{m}_f(u(\sigma))d\sigma + \\ \int_{t+\Delta t}^{t_f} \dot{m}_f(u(\sigma))d\sigma + h(SOC(t_f)) \} \end{aligned} \tag{13}$$

where Δt is a finite future time horizon. Bellman's principle of optimality ([8]) requires that,

$$\begin{aligned} J^*(SOC(t),t) = \min_{\substack{u(\tau) \\ t\le\tau\le t+\Delta t}} \{ \int_{t}^{t+\Delta t} \dot{m}_f(u(\tau))d\tau + \\ J^*(SOC(t+\Delta t),t+\Delta t) \} \end{aligned} \tag{14}$$

The minimum fuel cost over the interval $[t+\Delta t, t_f]$, i.e. $J^*(SOC(t+\Delta t),t+\Delta t)$, is not in general a known function of SOC. In the next section, we show how this function can be approximated enabling us to solve the above fuel minimization problem in a receding horizon approach.

IV. Minimum Fuel Cost-To-Go Approximation

In this section, we attempt to derive an approximation for the minimum fuel cost as a function of the battery's state of charge. An approximation of the cost-to-go will be sufficient, because the optimal solutions are recalculated in a receding horizon manner at each time step.
First, Taylor series expansion of $J^*(SOC(t+\Delta t),t+\Delta t)$ around $SOC^*(t+\Delta t)$ yields,

$$\begin{aligned} J^*(SOC(t+\Delta t),t+\Delta t) = J^*(SOC^*(t+\Delta t),t+\Delta t) + \\ \frac{\partial J^*}{\partial SOC}(SOC^*(t+\Delta t),t+\Delta t)\cdot\Delta SOC + O(\Delta SOC^2) \end{aligned} \tag{15}$$

where $\Delta SOC = (SOC(t+\Delta t) - SOC^*(t+\Delta t))$. As shown in the Appendix I, by observing the relationship between the Pontryagin's minimum principle and HJB equations, if SOC^* denotes the optimal trajectory from current time t and initial state $SOC(t)$ to the end of the trip, we can rewrite equation (15) as follows,

$$J^*(SOC(t+\Delta t),t+\Delta t) \cong J^*(SOC^*(t+\Delta t),t+\Delta t)+ \lambda(SOC(t),t)\cdot(SOC(t+\Delta t)-SOC^*(t+\Delta t)) \quad (16)$$

where,

$$\lambda(SOC(t),t) = \frac{\partial J^*}{\partial SOC}(SOC(t),t) \quad (17)$$

Adding and subtracting the constant reference value SOC_r, to the last term of equation (16) we obtain,

$$J^*(SOC(t+\Delta t),t+\Delta t) \cong \alpha(SOC(t),t)+ \lambda(SOC(t),t)\cdot(SOC(t+\Delta t)-SOC_r) \quad (18)$$

where, $\alpha(SOC(t),t)$ is defined by,

$$\alpha = J^*(SOC^*(t+\Delta t),t+\Delta t)+ \lambda(SOC(t),t)\cdot(SOC_r-SOC^*(t+\Delta t)) \quad (19)$$

Substituting (18) into cost function (14) we get,

$$J^*(SOC(t),t) = \min_{\substack{u(\tau)\\ t\le\tau\le t+\Delta t}} \{\alpha(SOC(t),t) + \int_t^{t+\Delta t} \dot{m}_f(u(\tau))d\tau+ \lambda(SOC(t),t)\cdot(SOC(t+\Delta t)-SOC_r)\} \quad (20)$$

Since α in (19) is not a function of the control inputs, it does not affect the selection of the optimal control inputs. So the optimal control over the interval $[t \quad t+\Delta t]$ can be found by solving the following optimal control problem,

$$\begin{aligned} &\min_{\substack{u(\tau)\\ t\le\tau\le t+\Delta t}} \{\int_t^{t+\Delta t} \dot{m}_f d\tau + \lambda(SOC(t),t)\cdot(SOC(t+\Delta t)-SOC_r)\}\\ &\dot{SOC} = f(u(\tau),v(\tau)); SOC_0 = SOC(t)\\ &SOC_{\min} \le SOC(\tau) \le SOC_{\max}, u(\tau)\in U \end{aligned} \quad (21)$$

where U is the set of admissible inputs according to (8). We will solve this finite-horizon optimal control problem in a receding horizon manner as explained in the next section.

As shown in Appendices I and II, the parameter λ is related to both the equivalent factor in the ECMS method and the rate of change of minimum cost with respect to the SOC. An admissible range for λ can be obtained as explained in the ECMS literature ([15]) or from the DP solutions over different driving cycles ([9]). In what follows, it is shown that λ can be approximated by a tunable piecewise linear function over its admissible range. Using equation (17), the Taylor series expansion of the function λ around the SOC_r yields,

$$\lambda(SOC(t),t) = \frac{\partial J^*}{\partial SOC}(SOC_r,t)+ \frac{\partial^2 J^*}{\partial SOC^2}(SOC_r,t)(SOC(t)-SOC_r)+O(\Delta SOC_r^2) \quad (22)$$

where $\Delta SOC_r = (SOC(t)-SOC_r) \ll 1$. By defining $\lambda_0 = \frac{\partial J^*}{\partial SOC}(SOC_r,t)$ and $\mu = \frac{\partial^2 J^*}{\partial SOC^2}(SOC_r,t)$ as two tuning design parameters and ignoring the higher order terms we obtain,

$$\lambda(SOC(t),t) \cong \lambda_0 + \mu\Delta SOC_r \quad (23)$$

which approximates λ as linearly dependent on the state.

V. Nonlinear MPC (NMPC) Energy Management

The discrete-time optimal control problem in (21) is first discretized with a fixed sampling time and solved in a receding horizon manner using dynamic programming. More specifically the following steps are carried out:

- At each step k, all the constraints are updated using the feedbacks from the plant model or HEV.
- The future power demand and vehicle speed (measured disturbances) are unknown over the prediction horizon. The future driver torque demand is assumed to be exponentially decreasing over the prediction horizon, i.e.

$$T_{driver}(k+i) = T_{driver}(k)e^{\left(\frac{-i\tau}{\tau_d}\right)} \qquad i = 1,\ 2,\ \cdots,\ P \quad (24)$$

  where $T_{driver}(k)$ is the known value of the driver torque demand at the beginning of the prediction horizon, τ is the sample time and τ_d determines the decay rate. The performance due to the choice of (24) has been confirmed by the simulation results. By using the above torque model and the vehicle longitudinal dynamics (6), the vehicle velocity profile over the prediction horizon is estimated.
- Using DP, the updated MPC problem (21) is solved numerically over the prediction horizon. Since the MPC horizon is short with respect to the whole cycle, the computations can be done in real-time.
- Consistent with standard MPC framework, only the first input in the sequence of the calculated optimal inputs over the horizon is applied to the plant and the above steps are repeated by receding the prediction horizon one step forward. Repeating these calculations for every new measurement yields a state feedback control law.

VI. Simulation model and control parameters

The power management module of a power-split HEV determines the engine, generator, motor, and friction brake torques based on the driver's demanded torque and the feedbacks from the vehicle. In this work, the control system is decomposed to two levels. The first or supervisory level is the MPC which finds the optimum values for the engine speed and engine torque. These optimum values are issued as references to the second or low-level controller. The low-level controller determines the engine, motor, generator, and friction brake torques required to follow the references set by the supervisory layer. A block-diagram of this system is shown in Figure 2. In the low-level controller, standard control loops are used for reference tracking.

In order to analyze the performance of our MPC power management scheme on a high-fidelity dynamic model of a

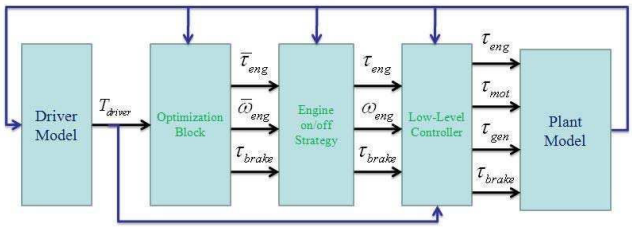

Fig. 2. Schematic of the control system architecture.

TABLE I

MPCs AND PSAT RESULTS (DRIVE CYCLES FROM [7])

UDDS cycle			
Controller	*Initial SOC*	*Final SOC*	*FuelEconomy (mpg)*
LTV MPC	0.70	0.59	84.31
	0.59	0.59	73.02
PSAT	0.70	0.67	78.55
	0.67	0.67	76.03
NMPC	0.70	0.68	82.37
	0.68	0.68	80.1
Highway FET cycle			
Controller	*Initial SOC*	*Final SOC*	*FuelEconomy (mpg)*
LTV MPC	0.70	0.63	70.1
	0.63	0.63	66.12
PSAT	0.70	0.64	69.43
	0.63	0.63	65.52
NMPC	0.70	0.74	69.63
	0.74	0.74	72.2

power-split HEV, the PSAT Simulink model of Toyota Prius was chosen as the plant model for closed-loop simulations which has been validated against the production HEV ([11]). The adjustable parameters of the MPC include the cost functional parameter and prediction and control horizons. In addition, the time constant τ_d in the torque model equation (24) is another tuning parameter. In the simulations, the sampling period of the MPC is 1 second. Also, the prediction and control horizons are 5 steps, and $\tau_d = 1$ is used in the simulations. In both PSAT and MPC controllers, the SOC constraint and reference are defined by $0.60 \leq SOC \leq 0.80$ and $SOC_r = 0.70$, respectively.

VII. SIMULATION RESULTS AND DISCUSSION

To quantitatively demonstrate the validity of the MPC strategy, we ran simulations over different driving cycles and some of the results are presented in Figure 3 and in Table I. The table compares the fuel economy and the initial and final SOCs of our previous LTV MPC controller, of the base controller in the PSAT software, and of the nonlinear MPC controller in this paper. In order to remove the effect of different initial and final SOCs on the fuel economy, we ran the simulations over the same cycle multiple times until the system reached a charge balance in which the SOC at the beginning and at the end of the cycle are the same. The fuel economy values with equal initial and final SOCs are used to compare the performance of different controllers. It can be observed that over both city and highway driving cycles, the MPC controller performance is improved.

Also in Table II, the closed-loop model is simulated over multiple driving cycles and it can be observed that the developed MPC strategy consistently shows better fuel economy

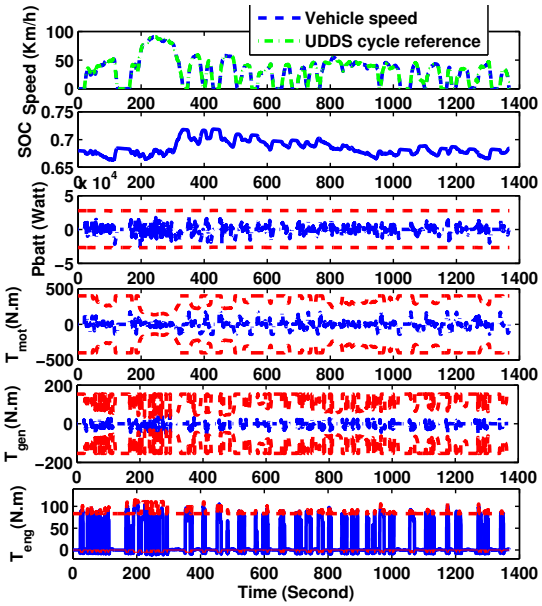

Fig. 3. The outputs and constraints of the NMPC closed-loop model over the UDDS cycle.

TABLE II

NMPC AND PSAT RESULTS (DRIVE CYCLES FROM [7])

US06 cycle			
Controller	*Initial SOC*	*Final SOC*	*FuelEconomy (mpg)*
PSAT	0.70	0.62	45.4
	0.6	0.6	42.8
NMPC	0.70	0.69	42.49
	0.69	0.69	46.01
SC03 cycle			
Controller	*Initial SOC*	*Final SOC*	*FuelEconomy (mpg)*
PSAT	0.70	0.68	71.29
	0.68	0.68	69
NMPC	0.70	0.69	76.66
	0.69	0.69	74.77
JC08 cycle			
Controller	*Initial SOC*	*Final SOC*	*FuelEconomy (mpg)*
PSAT	0.70	0.67	85.67
	0.67	0.67	81
NMPC	0.70	0.71	82
	0.71	0.71	83.6
NY City cycle			
Controller	*Initial SOC*	*Final SOC*	*FuelEconomy (mpg)*
PSAT	0.70	0.66	68.68
	0.64	0.64	52.6
NMPC	0.70	0.67	66.47
	0.67	0.67	58.25

even if the same control model and tuning parameters are used in different simulations.

VIII. CONCLUSIONS

A nonlinear MPC approach was proposed for solving the fuel minimization problem of a power-split hybrid electric vehicle. The proposed approach is based on breaking the fuel cost for an entire trip into a receding horizon stage cost and an approximation of the minimum cost-to-go as a function of battery's state of charge, using the Principle of Optimality. The breakdown to a short-horizon cost function allows to solve the fuel minimization problem effectively in real-time while considering the nonlinearities in the cost, dynamics, and constraints. The proposed method is systematic in both design and tuning and predictive in nature. The results over

a PSAT closed-loop model of a power-split HEV show that with this new approach, the fuel economy is improved noticeably with respect to that of an available controller in the commercial PSAT software and to the linear time-varying MPC controller developed in the past by the authors [5].

APPENDIX I
THE MINIMUM PRINCIPLE AND HEV FUEL MINIMIZATION

The necessary conditions for the optimality can be obtained by applying the variational approach (Pontriagin minimum principle [8]) to the fuel minimization problem. To do that, the Hamiltonian is,

$$H(SOC(\tau),u(\tau),p(\tau),\tau) = \dot{m}_f(u(\tau)) + p(\tau)[f^c(u(\tau),\tau)] \tag{25}$$

where $t \leq \tau \leq t_f$. Using this notation, the necessary conditions for the optimality from current time t and an initial value of $SOC(t)$ to the end of the drive cycle are,

$$\begin{aligned} &H = \dot{m}_f(u(\tau)) + p(\tau)[f^c(u(\tau),\tau)] = H(u(\tau),p(\tau),\tau) \\ &\dot{SOC}^*(\tau) = \tfrac{\partial H}{\partial p}(u^*(\tau),p^*(\tau),\tau) \\ &\dot{p}^*(\tau) = -\tfrac{\partial H}{\partial SOC}(u^*(\tau),p^*(\tau),\tau) = 0 \\ &H(SOC^*(\tau),u^*(\tau),p^*(\tau),\tau) \leq H(SOC^*(\tau),u(\tau),p^*(\tau),\tau) \end{aligned} \tag{26}$$

These conditions need to be satisfied for all admissible $u(\tau)$ in $t \leq \tau \leq t_f$. Since $\frac{\partial H}{\partial SOC} = 0$, we have $p^*(\tau) = \lambda(SOC(t),t)$. The relationship between HJB equations and the minimum principle implies that ([8]),

$$p^*(\tau) = \frac{\partial J^*(SOC^*(\tau),\tau)}{\partial SOC} = \frac{\partial J^*(SOC(t),t)}{\partial SOC} = \lambda(SOC(t),t) \tag{27}$$

Thus for an initial time, t, and a state of the charge, $SOC(t)$, by replacing $\tau = t + \Delta t$ we get

$$\frac{\partial J^*}{\partial SOC}(SOC^*(t+\Delta t),t+\Delta t) = \frac{\partial J^*}{\partial SOC}(SOC(t),t) \tag{28}$$

where $\frac{\partial J^*}{\partial SOC}(SOC(t),t) = \lambda(SOC(t),t)$. Notice that $SOC^*(\tau)$ is derived by relaxing the constraints which are enforced online by MPC along the finite prediction horizon.

APPENDIX II
THE PARAMETER OF THE MPC COST FUNCTIONAL AND THE ECMS FACTOR

In the ECMS method, an instantaneous cost function is defined by [2], [16],

$$J = \dot{m}_f(t) + S \cdot \frac{Pbatt(t)}{H_f} \tag{29}$$

where S is the ECMS factor. In Appendix I, the Hamiltonian is,

$$H = \dot{m}_f(u(t)) + p(t)\dot{SOC}(t) \tag{30}$$

According to the Pontryagin's Minimum Principle, [8],

$$J = H(SOC(t),u(t),p^*(t),t) = \dot{m}_f(u(t)) + p^*(t)\dot{SOC}(t) \tag{31}$$

By considering the dynamics of the battery and ignoring the power losses due to the internal resistance,

$$\dot{SOC}(t) \cong -\frac{P_{batt}}{C_{batt}V_{oc}}. \tag{32}$$

Hence it can be implied that,

$$p^*(t) = \left(\frac{C_{batt}V_{oc}}{H_f}\right) \cdot S \tag{33}$$

From the relationship between HJB equation and the minimum principle ([8]), it is obtained that,

$$\lambda(SOC(t),t) = p^*(t) = \left(\frac{C_{batt}V_{oc}}{H_f}\right) \cdot S \tag{34}$$

ACKNOWLEDGEMENTS

This project is supported by an URP grant from Ford Motor Company. Also, the authors wish to thank Dr. Ilya V. Kolmanovsky of University of Michigan for his valuable comments and discussions.

REFERENCES

[1] Antonio Sciarretta and Lino Guzzella, "Control of hybrid electric vehicles," *IEEE Control System Magazine*, pp. 60–67, Apr. 2007.

[2] G. Paganelli, S. Delprat, T. M. Guerra, J. Rimaux and J. J. Santin, "Equivalent consumption minimization strategy for parallel hybrid powertrains," *Proceedings of the Vehicular Technology Conference*, vol. 4, pp. 2076– 2081, 2002.

[3] C. Musardo, G. Rizzoni and B. Staccia, "A-ECMS: An adaptive algorithm for hybrid electric vehicle energy management," *Proceedings of the IEEE Conference on Decision and Control*, pp. 1816– 1823, 2005.

[4] G. Paganelli, S. Delprat, T.M. Guerra, J. Rimaux, and J.J. Santin, "Equivalent consumption minimization strategy for parallel hybrid powertrains," *Vehicular Technology Conference*, vol. 4, pp. 2076–2081, 2002.

[5] H. Borhan, A. Vahidi, A. Phillips, M. Kuang and I. Kolmanovsky, "Predictive energy management of a power-split hybrid electric vehicle," *American Control Conference*, pp. 3970 – 3976, 2009.

[6] P. Falcone, F. Borrelli, H. E. Tseng, J. Asgari and D. Hrovat, "Linear time-varying model predictive control and its application to active steering systems: Stability analysis and experimental validation," *International Journal of Robust and Nonlinear Control*, vol. 18, no. 8, pp. 1172–1177, 2004.

[7] Argonne National Laboratory, "Powertrain System Analysis Toolkit (PSAT) documentation," commercial software.

[8] Donald E. Kirk, "Optimal control theory an introduction," 2004.

[9] L. Johannesson, S. Pettersson, and B. Egardt, "Predictive energy management of a 4qt series-parallel hybrid electric bus," *Control Engineering Practice*, vol. 17, pp. 1440–1453, 2009.

[10] G. Zini, J. Kern, J. and M. Duoba, "Honda insight validation using PSAT," *SAE Paper 2001-01-2538*, 2001.

[11] A. Rousseau, J. Kwon, P. Sharer, S. Pagerit and M. Duoba, "Integrating data, performing quality assurance, and validating the vehicle model for the 2004 Prius using PSAT," *SAE Paper 2006-01-0667*, 2006.

[12] J. Liu and H. Peng, "Modeling and control of a power-split hybrid vehicle," *IEEE Transactions on Control Systems Technology*, vol. 16, no. 6, pp. 1242 – 1251, 2008.

[13] F. U. Syed, M. L. Kuang, J. Czubay and H. Ying, "Derivation and experimental validation of a power-split hybrid electric vehicle model," *IEEE Transactions on Control Systems Technology*, vol. 54, no. 6, pp. 1731–1747, 2006.

[14] M. Ehsani, Y. Gao, S. E. Gay and A. Emadi, *Modern Electric, Hybrid Electric, and Fuel Cell Vehicles: Fundamentals, Theory, and Design*, CRC, 2004.

[15] L. Guzzella and A. Sciarretta, *Vehicle Propusion Systems:Introduction to Modeling and Opitmization*, Springer, 2005, pp.190-203.

[16] L. Serrao, S. Onori, and G. Rizzoni, "ECMS as a realization of pontryagin's minimum principle for HEV control," *American Control Conference, 2009. ACC '09.*, pp. 3964 –3969, 2009.